THE JOURNAL OF BIOLOGICAL CHEMISTRY
Vol. 276, No. 48, Issue of November 30, pp. 44970–44975, 2001

Printed in U.S.A.

A Three-dimensional Model of the Human Facilitative Glucose Transporter Glut1*

Received for publication, August 1, 2001, and in revised form, September 20, 2001
Published, JBC Papers in Press, September 24, 2001, DOI 10.1074/jbc.M107350200

Felipe A. Zuniga‡, Guangpu Shi‡, Jorge F. Haller‡, Andrey Rubashkin‡, Diana R. Flynn‡, Pavel Iserovich‡, and Jorge Fischbarg‡§¶

From the Departments of §Physiology and ‡Ophthalmology, College of Physicians & Surgeons, Columbia University, New York, New York 10032

The human facilitative transporter Glut1 is the major glucose transporter present in all human cells, has a central role in metabolism, and is an archetype of the superfamily of major protein facilitators. Here we describe a three-dimensional structure of Glut1 based on helical packing schemes proposed for lactose permease and Glut1 and predictions of secondary structure, and refined using energy minimization, molecular dynamics simulations, and quality and environmental scores. The Ramachandran scores and the stereochemical quality of the structure obtained were as good as those for the known structures of the KcsA K^+ channel and aquaporin 1. We found two channels in Glut1. One of them traverses the structure completely, and is lined by many residues known to be solvent-accessible. Since it is delimited by the QLS motif and by several well conserved residues, it may serve as the substrate transport pathway. To validate our structure, we determined the distance between these channels and all the residues for which mutations are known. From the locations of sugar transporter signatures, motifs, and residues important to the transport function, we find that this Glut1 structure is consistent with mutagenesis and biochemical studies. It also accounts for functional deficits in seven pathogenic mutants.

The facilitative glucose transporter Glut1 is perhaps the most extensively studied membrane transporter. Over the last 15 to 20 years a number of technologies have been developed which have allowed investigators to observe and describe glucose transporter structure and function. Purification and reconstitution of the erythrocyte glucose transporter have allowed investigators to analyze its secondary structure using spectroscopic techniques (1, 2). Concurrently, the use of affinity labels such as phloretin, forskolin (3), and cytochalasin B (4, 5), group-specific chemical reagents (6, 7), proteases (8), and antibodies (8) have provided a topographical map of Glut1. cDNAs encoding the Glut1 protein have been isolated from human, rat, mouse, rabbit, and pig tissues (9–13). All encode proteins of 492 amino acids and all exhibit an extraordinarily high level of amino acid identity (~97%). Using hydropathy analysis, Glut1 was predicted by Mueckler and colleagues (9) to consist of 12 transmembrane-spanning α-helices with the N and C termini and a large loop between transmembrane helices 6 and 7 located on the cytoplasmic side of the membrane (9, 14–16). A smaller loop between transmembrane helices 1 and 2 was predicted to be extracellular (17). The bulk of experimental evidence to date supports this model. There are other Glut sugar transporter isoforms; of these, Glut2–5 have very high homology to Glut1, which suggests strong structural conservation between the different members of the family. By applying mutagenetic techniques to Glut1, selected conserved amino acids and whole domains have been altered, swapped, and deleted. The mutagenesis data have provided insight into locations, which are crucial for substrate binding and for conformational changes that result in D-glucose translocation (18). Glut1 admits dehydroascorbic acid as a substrate (19), and also exhibits a modest water conductance (20), suggesting the possible presence of a pore through the protein (9).

The lactose permease (lac permease)[1] of *Escherichia coli* (21, 22) and Glut1 are typical 12 transmembrane α-helical proteins of the major facilitator superfamily (23). Application to lac permease of cysteine scanning mutagenesis in conjunction with biochemical, biophysical, and immunological techniques has resulted in some 100 interactions mapped between residues in different helices. Based on the above, a helix-packing model of lac permease has been advanced (24, 25). In addition, from cysteine scanning mutagenesis of Glut1, Hruz and Mueckler (26, 27) and Keller and collegues (28, 29) have described residues related to glucose transport, and solvent accessible residues in helices II, V, VII, and XI. From this, a helix-packing model of Glut1 similar to that of lac permease has been suggested (27).

Our understanding of the sequence, biology, and biochemistry of Glut1 is increasing rapidly. However, given the attending difficulties in crystallizing membrane proteins, there is also growing interest in the development and application of molecular modeling techniques to understand the structure of Gluts and relate it to their function. The lack of crystallographic structures for most classes of membrane proteins (including Gluts) means that there are no suitable templates that can be used to generate structures by homology modeling. This creates a need for alternative modeling approaches in which the available experimental biological and biophysical data are used as a reference for the modeling process. The glucose transporter Glut1 is unique given the large amount of experimental data

* This work was supported by National Institutes of Health and Research to Prevent Blindness, Inc. Grant EY08918. The costs of publication of this article were defrayed in part by the payment of page charges. This article must therefore be hereby marked "*advertisement*" in accordance with 18 U.S.C. Section 1734 solely to indicate this fact.

The atomic coordinates and structure factors (code 1JA5) have been deposited in the Protein Data Bank, Research Collaboratory for Structural Bioinformatics, Rutgers University, New Brunswick, NJ (http://www.rcsb.org/).

¶ To whom correspondence should be addressed: Dept. of Physiology, College of Physicians & Surgeons, Columbia University, 630 West & 168th Street, New York, NY 10032. Tel.: 212-305-9092; Fax: 212-305-2461; E-mail: jf20@columbia.edu.

[1] The abbreviations used are: lac permease, lactose permease; pCMBS, *p*-chloromercuribenzenesulfonate; NEM, *N*-ethylmaleimide.

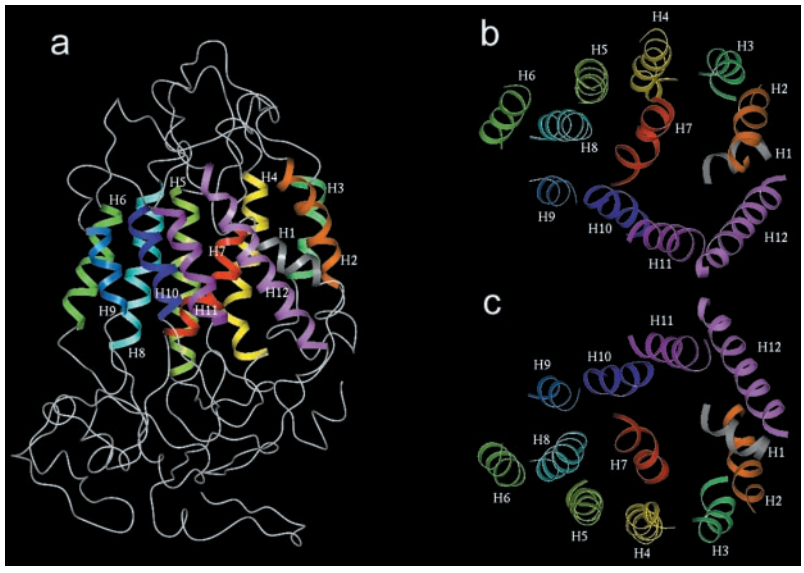

FIG. 1. **Ribbon representation of Glut1.** *a*, side view; helices are *colored*, and loops are *white*. The tilt of the 12 transmembrane helices, their relative positions, and the overall conformation are apparent. *b*, end-on view from the extracellular surface. *c*, end-on view from the cytoplasmic surface.

that are available. Therefore, starting from the helical packing schemes referred to above for lac permease and Glut1, we have been able to arrive at a three-dimensional structure of Glut1. We describe here the procedures utilized and offer validation for our structure using stereochemical analysis and mutagenesis data.

EXPERIMENTAL PROCEDURES

There are no crystallographic or NMR structure of any proteins with significant overall sequence similarity to Glut1 in the Research Collaboratory for Structural Bioinformatics Protein Data Bank. Thus we could not construct Glut1 by homology modeling. Instead, we chose to use a piecemeal strategy.

Helical Assignments—We used the GTR1_HUMAN sequence of Glut1 from Swiss Protein Data Base P11166. For the initial structure, α-helices were predicted using the consensus of the programs PHD (30), TMPRED (31), and PSA (32).

Modeling—For molecular modeling we utilized a Silicon Graphics Octane work station with InsightII software (Molecular Simulations, Inc.). The predicted helices were given the tilt and the three-dimensional proximity depicted in Kaback's scheme for lactose permease (24, 25). For the rotation around their z axis, we assumed that the helices were arranged with their hydrophilic sides facing a central channel. This was done based on deuterium exchange studies suggesting that 80% of the Glut1 backbone is accessible to water (1, 33), and on evidence that Glut1 has a modest but finite permeability to water (20, 34). For helices II, V, VII, and XI, the rotation was determined using the results of cysteine-scanning mutagenesis studies. For the rest of the helices, we used the results of Ducarme *et al.* (35) to determine the solvent-accessible faces. Loops were generated and connected using the "filgap" command in the program Whatif (36).

Refinement—The ensemble obtained was subject to energy minimization using the Discover module of InsightII (100 iterations with the steepest descent algorithm, and 1000 more with the conjugate gradients algorithm). By then, the root mean square derivative was <0.1 kcal mol^{-1} Å-1. We then used the program ProsaII (37) to assess and improve the locations of helical caps based on Prosa energy plots and Z-scores. The resulting residue assignments for the 12 α-helices are H1, 19–27; H2, 67–81; H3, 99–111; H4, 124–143; H5, 156–175; H6, 191–204; H7, 276–290; H8, 309–326; H9, 347–356; H10, 366–378; H11, 403–417; and H12, 424–445. At this stage of modeling, helical residues fell well into the most favored Ramachandran regions, but many loop residues fell in disallowed regions and exhibited close contacts (distances $<$ 2.2 Å) and undesirable torsion angles. We therefore searched for homologous loops with better conformations using the program Swiss-Pdb Viewer (V3.5) (38). The structure was then subjected to minimization as above, and to molecular dynamics (CVFF forcefield; 298 K; 5 ps of initial equilibration followed by 5 ps dynamics run) with the backbone fixed to optimize the position of the side chains.

TABLE I
PROCHECK Ramachandran scores for the structures of Glut1, the KcsA K^+ channel, and the AQP1 water channel

Structure	Ramachandran plot (%)			
	Core	Allowed	Generous	Disallowed
Glut1[a]	81.5	16.9	1.7	0.0
KCSA[b]	74.7	24.1	1.2	0.0
AQP1[c]	70.7	20.9	8.4	0.0

[a] Protein Data Bank number: 1JA5.
[b] Protein Data Bank number: 1BL8.
[c] Protein Data Bank number: 1IH5.

RESULTS AND DISCUSSION

A ribbon representation of the Glut1 structure we found is given in Fig. 1. Helices 1–5, 8, and 10–12 are arranged in a 9-member barrel-like manner, delimiting a hydrophilic central channel. Helix 7 projects itself into the channel, suggesting a central role in regulating putative transport of solutes through that channel. From the side view, the structure appears roughly symmetrical, as in other barrel proteins. The arrangement of the helices is conical, the shorter side facing exofacially. This may be related to the fact that, as a rule, the exofacial loops tend to be shorter than the endofacial ones.

The quality of the Glut1 structure was ascertained using the program PROCHECK (version 3.3.2) (39). For comparison, we also determined the quality of the structures reported for two α-helical membrane proteins solved by crystallography, the KcsA K^+ channel (40), and the aquaporin 1 (AQP1) water channel (41). Table I gives the distribution of the ϕ, ψ angles in the different regions of the Ramachandran plot. As can be seen, the Glut1 structure is at least as good as those of the other proteins. Several PROCHECK stereochemical parameters and the stereochemical quality are summarized in Table II. From this table, the quality of the Glut1 structure appears as good as (or better) that of two α-helical membrane proteins, the Kcsa and AQP1 channels, implying excellent structural quality for our model structure. To be noted, the PDB data base from which the loops were derived is composed overwhelmingly by globular proteins. It is unclear whether the standard quality factors for facilitator/channel membrane proteins would be precisely the same as those for globular ones, as facilitators/channels would be expected to include a water-filled internal pore in their fold. Hence, that the quality of our structure may appear "better" than those of the comparison channels may be simply related to the data base peculiarity noted.

TABLE II
Summary of PROCHECK quality assessment (63) data

Structure	H-bond energy S.D.	Bad contacts per 100 residues	χ_{-1} pooled SD	Stereochemical quality index[a]		
				ϕ, ψ Distribution	χ_1 S.D.	HB energy
Glut1	0.87	1.2	20.9	1	3	2
KCSA	1.0	6.7	23.2	2	3	3
AQP1	0.8	7.6	30.8	2	4	3

[a] Quality index: 1 highest.

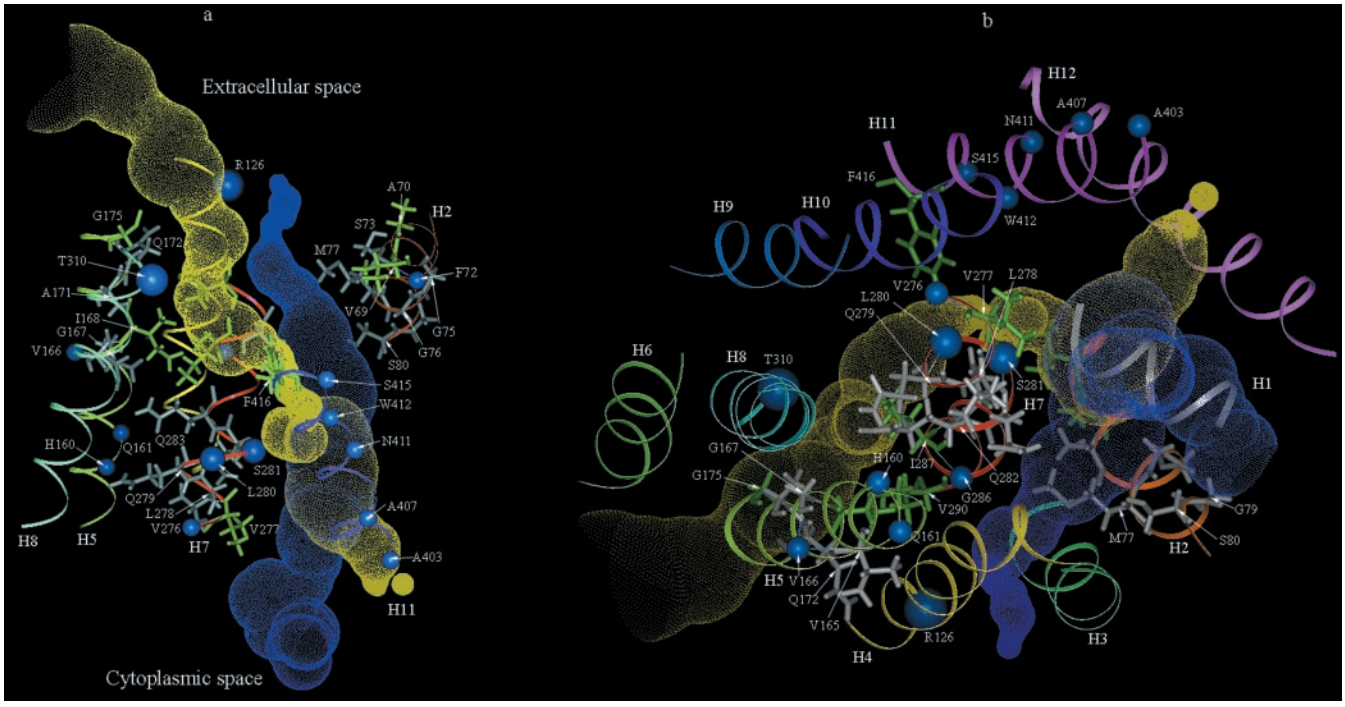

FIG. 2. **Ribbon representation of Glut1 with a space filling representation of the main channel (in *yellow*) and the auxiliary channel (in *blue*).** Helices are *colored* and loops are *white*, as in Fig. 1. *a*, side view, showing helices 2, 4, 5, 7, 8, and 11. All loops and the other helices are omitted for clarity. *b*, end-on view from the cytoplasmic surface; loops omitted. Residue representations are: *large blue balls*, sites of pathogenic mutations; *medium blue balls*, QLS motif; *small blue balls*, essential for glucose transport; *green sticks*, sensitive to mercurials NEM or/and pCMBS; *gray sticks*, both essential for glucose transport and mercurial sensitive.

We next sought to determine if our structure agrees with the functional and biochemical characteristics experimentally determined for Glut1 by many laboratories. Using the program HOLE (42), we looked for solvent-accessible channels that might serve as transport pathways. We find two channels in our structure. One (the main one) traverses both α-helical and loop regions, and passes close to and curls around helix 7 (*cf.* Figs. 2 and 3). This channel could serve as the glucose transport channel, as elaborated below. The second one (auxiliary channel) is delimited by helices 1, 2, 3, and 7; it is open only at the endofacial site, where it overlaps with the main channel. A study by Keller's (29) laboratory concluded there is an exofacial solvent accessible cleft between helices 2 and 7, and that such a cleft could serve as a pathway for substrates other than sugars. The presence of the auxiliary channel in our structure is consistent with such conclusion. In addition, the existence of two solvent-filled channels in the Glut1 structure is also supported by the deuterium exchange studies cited above suggesting that 80% of the Glut1 backbone is accessible to water (1, 33).

In Fig. 2 we show the relationships between main channel and auxiliary channel with several residues known to be pathogenic mutations (**bold**), or essential for glucose transport function (*italics*), or mercurial-sensitive (underlined), or both essential for transport and mercurial-accessible (*italics underlined*). The main channel enters the 12 α-helical domain close to residues **Thr^{310}** (43) (H8), *Gly^{175}* (H5), and to H7. The figure then shows the proximity of the channel to H7 and residues *Gln^{172}*, *Val^{290}*, *Phe^{416}*, *Ile^{287}*, and *Asn^{288}*. About midway, the main channel turns toward H2 (Fig. 2*b*), passing close to *Ser^{80}*, *Leu^{280}*, *Ser^{281}*, and *Gln^{282}*. It then turns once more and goes toward the cytoplasmic side passing near *Leu^{278}*, *Val^{277}*, and *Val^{276}*. The channel has two segments joined by a bottleneck region near the level of the QLS motif. As Fig. 2 shows, H7, H8, and H11 are all crucial components of the channel. Interestingly, this organization is strikingly reminiscent of the one in a Glut1 model suggested by Jung and colleagues (44). Of the two Glut1 models offered there, both of them had H7, H8, and H11 forming part of the channel, as in this one. While on the subject of Glut models, importantly, D. S. Dwyer (45) has recently described a three-dimensional model for Glut3, which is the major glucose transporter of neuronal cells and is highly homologous to Glut1. Dwyer arrived at his structure differently than ourselves. He used homology modeling on the basis of structural data from the MscL protein, a mechanosensititive ion channel, and general insights from aquaporin 1. A detailed comparison of his model with our current one cannot be offered, as no three-dimensional coordinates for Dwyer's model have appeared in the PDB data base at this writing. In broad terms, in Dwyer's approach, functional correlations with Glut3 residues at equivalent positions of Glut1 mutants are unclear, the pore appears somewhat narrower than that in our model (perhaps as a result of his assumption that only 6 helices limit the pore), and the fold of his long intracellular segment is more

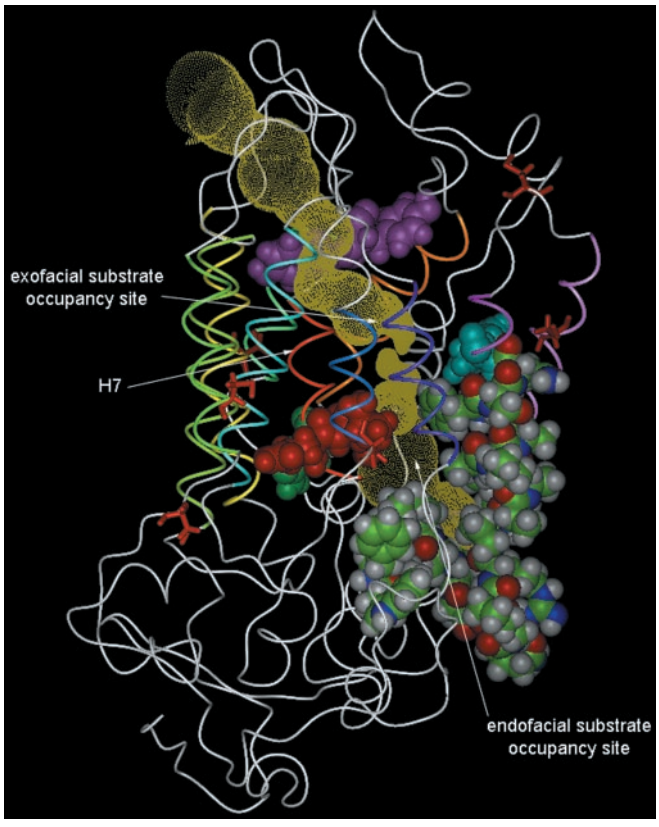

FIG. 3. **Ribbon representation of Glut1 with a space-filling representation of the main channel (in *yellow*).** Helices are *colored* and loops are *white*, as in Fig. 1. Residues in space-filling rendering correspond to several conserved motifs around the channel; Gln^{279}, Leu^{280}, Ser^{281} (QLS motif) are *red*, Tyr^{292} and Tyr^{293} are *purple*; Gln^{282}, *green*; and Trp^{412}, *cyan*. Residues 388–412 implicated in the putative binding site for cytochalasin B are colored by atom. Last, all cysteines are shown as *sticks* in *red*.

TABLE III
Not accessible to pCMBS, far from channel, but changes activity

Amino acid	Distance to channel
	Å
Ser^{80}	11.10
Leu^{156}	11.29
His^{160}	9.84
Gln^{161}	17.79
Gln^{279}	12.81
Ala^{403}	9.79
Ala^{407}	10.27
Asn^{411}	11.30
Phe^{422}	17.19

TABLE IV
Not accessible to pCMBS but near channel and important for activity

Amino acid	Distance to channel
	Å
Val^{83}	3.40
Gln^{282}	4.85
Leu^{284}	On the channel
Asn^{288}	On the channel
Tyr^{292}	3.10
Trp^{412}	3.33

TABLE V
Accessible to pCMBS or NEM

Amino acid	Distance to channel
	Å
Thr^{62}	5.13
Ile^{168}	5.69
Ala^{171}	3.41
Gln^{172}	5.86
Gln^{175}	2.52
Leu^{273}	3.42
Ile^{274}	2.50
Val^{277}	2.84
Ile^{278}	5.79
Leu^{280}	4.54
Ser^{281}	On the channel
Ile^{287}	On the channel
Val^{290}	1.16
Phe^{291}	On the channel
Tyr^{293}	4.88
Ser^{294}	On the channel
Ala^{289}	6.56

TABLE VI
Accessible to pCMBS, forming cleft in helix 2

Amino acid	Distance to auxiliary channel
	Å
Ser^{66}	9.86
Ala^{70}	9.30
Ser^{73}	7.86
Gly^{75}	7.39
Gly^{76}	4.04
Met^{77}	On the channel
Gly^{79}	5.42

TABLE VII
Not accessible to pCMBS; no change in activity

Amino acid	Distance to channel	Amino acid	Distance to channel
	Å		Å
Thr^{63}	7.54	Val^{166}	13.44
Leu^{64}	11.53	Leu^{169}	12.29
Leu^{67}	15.74	Ile^{170}	10.70
Ser^{68}	14.43	Val^{173}	8.02
Val^{69}	7.47	Phe^{174}	7.78
Ile^{71}	21.44	Ile^{272}	9.50
Val^{74}	16.50	Ala^{275}	11.29
Ile^{78}	17.00	Val^{276}	8.71
Phe^{81}	17.00	Ser^{285}	8.54
Ser^{82}	10.83	Gly^{286}	6.72
Gly^{84}	8.93	Val^{406}	10.57
Leu^{85}	22.15	Ser^{410}	9.27
Phe^{86}	25.58	Thr^{413}	7.96
Val^{87}	12.30	Ser^{414}	11.09
Gly^{157}	12.02	Asn^{415}	7.55
Thr^{158}	14.28	Ile^{417}	11.31
Leu^{159}	16.50	Val^{418}	12.18
Leu^{162}	20.72	Met^{420}	9.45
Gly^{163}	16.20	Cys^{421}	15.78
Ile^{164}	10.21	Phe^{422}	17.19

extended than ours. On the other hand, in the molecular dynamics he presents, glucose does move 3.5 Å along the pore. In addition, although the helical tilts from the vertical appear less pronounced in his case, there is similarity with the overall packing of our own model (and Kaback's scheme) both in the relative positions of the helices and in the fact that his helix 7 also appears inside a large hydrophilic cavity and borders on the pore. Given the different starting points referred to, such similarity between the models appears quite significant.

To return to our structure, the exofacial segment of the main channel is surrounded by the periplasmic ends of H5, H7, H8, H9, and H10 (Figs. 1*b* and 2), and the endofacial segment by the cytoplasmic ends of H1, H2, H3, H7, and H11. Fittingly, there is evidence (26) that the periplasmic segments of H5 and H7 were accessible to extracellular pCMBS while their cytoplasmic segments were not. From Fig. 2, the main channel curls around H7, away from the cytoplasmic portion of H5, and

TABLE VIII
Cysteine locations

Amino acid	Distance to channel
	Å
Cys^{133}	11.08
Cys^{201}	28.91
Cys^{207}	22.59
Cys^{347}	12.00
Cys^{421}	16.89
Cys^{429}	12.22

TABLE IX
Accessible to pCMBS, located far from channel

Amino acid	Distance to channel
	Å
Trp^{65a}	9.47
Gly^{167}	10.00
Gln^{283}	11.50
Gly^{419b}	10.79
Cys^{429}	12.22

[a] On loop I.
[b] On loop XI.

TABLE X
Not accessible to pCMBS, not important for activity, located near channel

Amino acid	Distance to channel
	Å
Ser^{118}	5.57
Leu^{176}	On the channel
Ser^{178}	5.00
Thr^{295}	1.73
Ser^{296}	On the channel
Ile^{297}	2.82
Ala^{402}	5.72
Ile^{404}	On the channel
Ala^{405}	2.43
Gly^{408}	5.71
Phe^{409}	On the channel

TABLE XI
Pathogenic mutations

Amino acid	Distance to channel
	Å
S66F[a]	11.45
R126L	On auxiliary channel
E146K[a]	7.47
K256W[a]	14.83
G272A[a]	10.17
T310I[a]	On the channel
R333W[a]	21.24

[a] Located on loops regions.

moving toward the opposite face of H7 as it forms its endofacial segment. Although the cytoplasmic portion of H7 is close to the endofacial segment of the channel, it is structurally not easily accessed by extracellular pCMBS because of the bottleneck. However, it can be accessed by NEM (26), as referred to below.

To investigate the location of the exofacial-binding site, we positioned a glucose molecule in the widest part of the exofacial segment of the main channel (not shown). During a subsequent 10-ps molecular dynamics simulation, the glucose molecule remained in that general area and formed a hydrogen bond to Asn^{288}. This is consistent with experimental evidence: the mutation N288C resulted in a 10-fold reduction in normalized glucose transport (27). It would appear that the minimized structure we have arrived at corresponds to or is near the so-called endofacial conformation. The exploration of putative intermediate conformations leading to an exofacial one will be the subject of future studies.

We next determined the spatial relations between the main channel in our structure and the locations of conserved residues and motifs, which are characteristic of the family of hexose transporters. From mutagenesis experiments, the conserved QLS motif in helix 7 forms part of the exofacial substrate-binding site and acts as a selectivity filter allowing Glut1, -3, and -4 to transport glucose, but not fructose (46). In our structure (Fig. 3), the QLS motif delimits the main channel (herein after channel) and is in the vicinity of the putative exofacial substrate occupancy site. Similarly, it is known that substitutions of the conserved residues $Tyr^{292/293}$, and Trp^{412} markedly affect transporter function (18). Fittingly, in our structure (Fig. 3), $Tyr^{292/293}$ delimit the channel, and Trp^{412} is in close proximity to it. Turning now to the cytochalasin B-binding site, evidence locates it somewhere near residues 388–412 (47). As highlighted in Fig. 3, those residues are very close to the endofacial end of both channels. Finally, it is known that none of the native Glut1 cysteine residues are essential for transport function (48). Once more, as Fig. 3 shows, the structure conforms to prior evidence: in our structure, all cysteines are far from the channel. From all this, our structure accounts very well for the experimental evidence this far.

There are studies suggesting that Glut1 in erythrocytes can exist as an oligomer with a putative disulfide bond between cysteine residues 347 and 421 (49). However, when the Glut1 construct with all the cysteine residues replaced (C-less Glut1 (48, 50)) is expressed in *Xenopus laevis* oocytes, glucose transport is practically unaffected. Moreover, other studies suggest the existence of monomeric functional Glut transporters (forms 1–3) with no alteration in the kinetic parameters when expressed in *X. laevis* oocytes (51). The significance of the polymeric nature of Gluts is an interesting, still unclear question. In contrast, as detailed in the context, using our model for a monomer we can explain the results of almost all the mutagenic studies done so far.

As a further test of our structure, we next sought to quantify the degree to which the locations of the channels in the structure correspond to those of all Glut1 94 residues which have been mutated (26–29, 50, 52–58). We investigated the relationship between the residue locations and the properties described for each residue as accessibility to pCMBS or NEM (defined as resulting in transport of <50%), and decrease in Glut1 transport activity (to <50%) concurrent with the mutations. For this, we measured the distances from each residue to given channels. Tables III-X describe these relationship grouping residues by their characteristics.

Table III shows residues that are far from the channel (d >9 Å) but still produce a decrease in transport activity when mutated. We would expect them not to be accessible to pCMBS, and they are not. The decrease could therefore result from changes in Glut1 structure that influence transport secondarily. Table IV lists residues that are close to the channel (d <5 Å), and affect transport activity, but are inaccessible to pCMBS. The proximity to the channel can account for the effect on transport; the inaccessibility to pCMBS may be due to steric impediments. Table V lists residues that are close to the channel and are accessible to pCMBS or to NEM, as might be expected. Table VI lists helix 2 residues accessible to pCMBS; several are located near or at the auxiliary channel. Table VII lists residues located far from the channel, therefore expected neither to be accessible to pCMBS, nor to affect transport activity, which the table shows to apply to all of them (silent mutations). Table VIII lists all 6 cysteines in Glut1. As mentioned above, all the native Glut1 cysteine residues can be

mutated without affecting transport (48), so one would expect them to be far from the channel. In agreement with this, $d > 11$ Å for all. In this connection, there is evidence that in single-Cys Glut1 mutants Cys^{201} or Cys^{429} expressed in oocytes, alkylation by external or internal pCMBS inhibits glucose transport (59). Several models locate these residues near the endofacial end of helix 6 and the exofacial end of 12, respectively, from which they would be accessible to pCMBS under the conditions of that study. Given their putative positions away from the transport channel, such alkylations might interfere with the conformational changes necessary for glucose transport (as previously suggested (59)).

Table IX lists four residues located far from the channel, but accessible to pCMBS. Still, Trp^{65} and Gly^{419} are in exofacial loops, so pCMBS could reach them. As for Gly^{167} (H5) and Gln^{283} (H7), the side chains are close to each other (3.0 Å) and next to the endofacial ends of their helices. Given the putative mobility of H7, accessibility to the mercurial could be explained on that basis. Table X list residues located near the channel, but not important for transport activity, and not accessible to pCMBS either. Steric factors or conformational changes could explain such behavior. Table XI lists (pathogenic) mutations that have been found to give rise to the De Vivo (60–62) (glucose transporter deficiency) neurological syndrome. Of these, residue 310 is on the main channel, and 126 is on the auxiliary channel, which may account for the pathogenicity noted. Residue 66 is in a loop next to the exofacial end of H2 and therefore near the cleft between H2 and H7, identified as important for transport function (29). Most interestingly, the other three residues (256, 272, and 333) are in intracellular loops, configure a triangle ($10.19 \times 10.01 \times 13.77$ Å between Cα atoms), and are located on both sides of a cleft which might be involved in binding an indispensable factor. In summary, these considerations appear to provide very strong validation for our structure. Of the mutant residues, in 88% the effects are very well accounted for by our structure, and for the other 12% explanations compatible with the structure can be given. This strengthens our present suggestion that the proposed model for Glut1 is not very far from the native structure of this protein.

Acknowledgment—We thank Dr. D. Dwyer for helpful suggestions.

REFERENCES

1. Alvarez, J., Lee, D. C., Baldwin, S. A., and Chapman, D. (1987) *J. Biol. Chem.* **262,** 3502–3509
2. Pawagi, A. B., and Deber, C. M. (1990) *Biochemistry* **29,** 950–955
3. Sergeant, S., and Kim, H. D. (1985) *J. Biol. Chem.* **260,** 14677–14682
4. Krupka, R. M., and Deves, R. (1986) *Biochem. Cell Biol.* **64,** 1099–1107
5. Basketter, D. A., and Widdas, W. F. (1978) *J. Physiol.* **278,** 389–401
6. Rampal, A. L., and Jung, C. Y. (1987) *Biochim. Biophys. Acta* **896,** 287–294
7. May, J. M. (1989) *Biochim. Biophys. Acta* **986,** 207–216
8. Takata, K., Kasahara, T., Kasahara, M., Ezaki, O., and Hirano, H. (1992) *Cell Tissue Res.* **267,** 407–412
9. Mueckler, M., Caruso, C., Baldwin, S. A., Panico, M., Blench, I., Morris, H. R., Allard, W. J., Lienhard, G. E., and Lodish, H. F. (1985) *Science* **229,** 941–945
10. Birnbaum, M. J., Haspel, H. C., and Rosen, O. M. (1986) *Proc. Natl. Acad. Sci. U. S. A.* **83,** 5784–5788
11. Kaestner, K. H., Christy, R. J., McLenithan, J. C., Braiterman, L. T., Cornelius, P., Pekala, P. H., and Lane, M. D. (1989) *Proc. Natl. Acad. Sci. U. S. A.* **86,** 3150–3154
12. Baldwin, S. A. (1993) *Biochim. Biophys. Acta* **1154,** 17–49
13. Asano, T., Shibasaki, Y., Kasuga, M., Kanazawa, Y., Takaku, F., Akanuma, Y., and Oka, Y. (1988) *Biochem. Biophys. Res. Commun.* **154,** 1204–1211
14. Cairns, M. T., Alvarez, J., Panico, M., Gibbs, A. F., Morris, H. R., Chapman, D., and Baldwin, S. A. (1987) *Biochim. Biophys. Acta* **905,** 295–310
15. Davies, A., Meeran, K., Cairns, M. T., and Baldwin, S. A. (1987) *J. Biol. Chem.* **262,** 9347–9352
16. Davies, A., Ciardelli, T. L., Lienhard, G. E., Boyle, J. M., Whetton, A. D., and Baldwin, S. A. (1990) *Biochem. J.* **266,** 799–808
17. Asano, T., Katagiri, H., Takata, K., Lin, J. L., Ishihara, H., Inukai, K., Tsukuda, K., Kikuchi, M., Hirano, H., and Yazaki, Y. (1991) *J. Biol. Chem.* **266,** 24632–24636
18. Barrett, M. P., Walmsley, A. R., and Gould, G. W. (1999) *Curr. Opin. Cell Biol.* **11,** 496–502
19. Vera, J. C., Rivas, C. I., Fischbarg, J., and Golde, D. W. (1993) *Nature* **364,** 79–82
20. Fischbarg, J., Kuang, K., Vera, J. C., Arant, S., Silverstein, S. C., Loike, J., and Rosen, O. M. (1990) *Proc. Natl. Acad. Sci. U. S. A.* **87,** 3244–3247
21. Kaback, H. R. (1997) *Proc. Natl. Acad. Sci. U. S. A.* **94,** 5539–5543
22. Kaback, H. R., Voss, J., and Wu, J. (1997) *Curr. Opin. Struct. Biol.* **7,** 537–542
23. Pao, S. S., Paulsen, I. T., and Saier, M. H. (1998) *Microbiol. Mol. Biol. Rev.* **62,** 1–34
24. Frillingos, S., Sahin-Toth, M., Wu, J., and Kaback, H. R. (1998) *FASEB J.* **12,** 1281–1299
25. Venkatesan, P., Liu, Z., Hu, Y., and Kaback, H. R. (2000) *Biochemistry* **39,** 10649–10655
26. Hruz, P. W., and Mueckler, M. M. (1999) *J. Biol. Chem.* **274,** 36176–36180
27. Hruz, P. W., and Mueckler, M. M. (2000) *Biochemistry* **39,** 9367–9372
28. Olswoski, A., Monden, I., and Keller, K. (1998) *Biochemistry* **37,** 10738–10745
29. Olswoski, A., Monden, I., Krause, G., and Keller, K. (2000) *Biochemistry* **39,** 2469–2474
30. Rost, B. (1996) *Methods Enzymol.* **266,** 525–539
31. Pasquier, C., Promponas, V. J., Palaios, G. A., Hamodrakas, J. S., and Hamodrakas, S. J. (1999) *Protein Eng.* **12,** 381–385
32. Stultz, C. M., White, J. V., and Smith, T. F. (1993) *Protein Sci.* **2,** 305–314
33. Jung, E. K., Chin, J. J., and Jung, C. Y. (1986) *J. Biol. Chem.* **261,** 9155–9160
34. Zhang, R., Alper, S., Thorens, B., and Verkman, A. S. (1991) *J. Clin. Invest.* **88,** 1553–1558
35. Ducarme, P., Rahman, M., Lins, L., and Brasseur, R. (1996) *J. Mol. Modeling* **2,** 27–45
36. Oliveira, L., Paiva, A. C., and Vriend, G. (1999) *Protein Eng.* **12,** 1087–1095
37. Sippl, M. J. (1993) *Proteins* **17,** 355–362
38. Guex, N., and Peitsch, M. C. (1997) *Electrophoresis* **18,** 2714–2723
39. Laskowki, R. A., MacArthur, M. W., Moss, D. S., and Thornton, J. M. (1993) *J. Appl. Crystallog* **26,** 283–291
40. Doyle, D. A., Cabral, J. M., Pfuetzner, R. A., Kuo, A., Gulbis, J. M., Cohen, S. L., Chait, B. T., and MacKinnon, R. (1998) *Science* **280,** 69–77
41. Ren, G., Reddy, S., Cheng, A., Melnyk, P., and Mitra, A. K. (2001) *Proc. Natl. Acad. Sci. U. S. A.* **98,** 1398–1403
42. Smart, O. S., Goodfellow, J. M., and Wallace, B. A. (1993) *Biophys. J.* **65,** 2455–2460
43. Klepper, J., Wang, D., Fischbarg, J., Vera, J. C., Jarjour, I. T., O'Driscoll, K. R., and De Vivo, D. C. (1999) *Neurochem. Res.* **24,** 587–594
44. Zeng, H., Parthasarathy, R., Rampal, A. L., and Jung, C. Y. (1996) *Biophys. J.* **70,** 14–21
45. Dwyer, D. S. (2001) *Proteins* **42,** 531–541
46. Seatter, M. J., De la Rue, S. A., Porter, L. M., and Gould, G. W. (1998) *Biochemistry* **37,** 1322–1326
47. Holman, G. D., and Rees, W. D. (1987) *Biochim. Biophys. Acta* **897,** 395–405
48. Wellner, M., Monden, I., and Keller, K. (1995) *FEBS Lett.* **370,** 19–22
49. Zottola, R. J., Cloherty, E. K., Coderre, P. E., Hansen, A., Hebert, D. N., and Carruthers, A. (1995) *Biochemistry* **34,** 9734–9747
50. Mueckler, M., and Makepeace, C. (1997) *J. Biol. Chem.* **272,** 30141–30146
51. Burant, C. F., and Bell, G. I. (1992) *Biochemistry* **31,** 10414–10420
52. Wellner, M., Monden, I., and Keller, K. (1992) *FEBS Lett.* **309,** 293–296
53. Garcia, J. C., Strube, M., Leingang, K., Keller, K., and Mueckler, M. M. (1992) *J. Biol. Chem.* **267,** 7770–7776
54. Katagiri, H., Asano, T., Ishihara, H., Lin, J. L., Inukai, K., Shanahan, M. F., Tsukuda, K., Kikuchi, M., Yazaki, Y., and Oka, Y. (1993) *Biochem. J.* **291,** 861–867
55. Mueckler, M., Weng, W., and Kruse, M. (1994) *J. Biol. Chem.* **269,** 20533–20538
56. Tamori, Y., Hashiramoto, M., Clark, A. E., Mori, H., Muraoka, A., Kadowaki, T., Holman, G. D., and Kasuga, M. (1994) *J. Biol. Chem.* **269,** 2982–2986
57. Mori, H., Hashiramoto, M., Clark, A. E., Yang, J., Muraoka, A., Tamori, Y., Kasuga, M., and Holman, G. D. (1994) *J. Biol. Chem.* **269,** 11578–11583
58. Mueckler, M., and Makepeace, C. (1999) *J. Biol. Chem.* **274,** 10923–10926
59. Wellner, M., Monden, I., and Keller, K. (1994) *Biochem. J.* **299,** 813–817
60. Klepper, J., Fischbarg, J., Vera, J. C., Wang, D., and De Vivo, D. C. (1999) *Pediatr. Res.* **46,** 677–683
61. Wang, D., Kranz-Eble, P., and De Vivo, D. C. (2000) *Hum. Mutat.* **16,** 224–231
62. Klepper, J., Willemsen, M., Verrips, A., Guertsen, E., Herrmann, R., Kutzick, C., Florcken, A., and Voit, T. (2001) *Hum. Mol. Genet.* **10,** 63–68
63. Morris, A. L., MacArthur, M. W., Hutchinson, E. G., and Thornton, J. M. (1992) *Proteins* **12,** 345–364